

Reduction of the Surface Roughness Induced Spin Relaxation in SOI Structures: An Analytical Approach

Dmitri Osintsev^{1,2}, Victor Sverdlov¹, and Siegfried Selberherr¹

¹Institute for Microelectronics, TU Wien, Gußhausstraße 27-29, A-1040 Wien, Austria

²Volgograd State Technical University, Lenin Avenue 28, 400131 Volgograd, Russia

Email: {Osintsev/Sverdlov/Selberherr}@iue.tuwien.ac.at

1. Introduction

Spintronics attracts at present much interest because of the potential to build novel spin-based devices which are superior to nowadays charge-based electronics. Silicon is composed of nuclei with predominantly zero spin and it is characterized by small spin-orbit coupling. Both factors favour to reduce spin relaxation. Understanding the details of the spin propagation in silicon structures is urgently needed [1]. We investigate the surface roughness induced spin scattering and relaxation matrix elements in silicon-on-insulator-based spin field-effect transistors by applying an analytical approach. We demonstrate that shear strain dramatically influences the spin, opening a new opportunity to boost spin lifetime in silicon spin field-effect transistors.

2. Method and Results

In this work we investigate the influence of the intrinsic spin-orbit interaction on the subband structure, spin scattering, and spin relaxation matrix elements due to surface roughness. The $\mathbf{k}\cdot\mathbf{p}$ Hamiltonian (1) was obtained by changing the basis of the generalized Hamiltonian which includes the spin degree of freedom [2-4]. The Hamiltonian is written in the vicinity of the X point along the k_z axis in the Brillouin zone. m_t and m_l are the transversal and the longitudinal silicon effective masses, $k_0 = 0.15 \times 2\pi/a$ is the position of the valley minimum relative to the X point in unstrained silicon, ε_{xy} denotes the shear strain component, $M^{-1} \approx m_t^{-1} - m_0^{-1}$, $D = 14\text{eV}$ is the shear strain deformation potential, and $\Delta_{SO} = 1.27\text{meVnm}$.

Four wave functions are considered: $X_{1\uparrow}$, $X_{1\downarrow}$, $X_{2\uparrow}'$, $X_{2\downarrow}'$, for the lowest spin up, spin down and for the second conduction band spin up, spin down, respectively. The transformations (1) are applied to get rid of the coupling between the spins with opposite direction in different valleys. Following [3] we then found the wave functions in the same manner as for the two-band $\mathbf{k}\cdot\mathbf{p}$ Hamiltonian written in the vicinity of the X point of the Brillouin zone for silicon films under uniaxial strain.

The surface roughness scattering between the subbands is taken to be proportional to the square of the product of the subband wave function derivatives at the interface [5]. Figure 1 demonstrates an excellent

agreement between the analytical solution and the numerically obtained results for a silicon film of 4nm thickness for the values $k_x = 0.25\text{nm}^{-1}$ and $k_y = 0.25\text{nm}^{-1}$. For the numerical calculations a barrier of 10eV height has been assumed.

Figure 2 shows energies in the first subband for different values of the wave vector \mathbf{k} and minimum energy in the second valley that is achieved for $\mathbf{k} = 0$. Intraband scattering is only possible, when the energy in the second subband is less or equal to the energy in the first subband.

The dependence of the intersubband scattering matrix elements on shear strain is shown in Figure 3. The minimum in the intersubband scattering is achieved, when the term $D\varepsilon_{xy} - \frac{\hbar^2 k_x k_y}{M} = 0$. Intersubband scattering vanishes, when the kinetic energy is not sufficient to have scattering states in the second subband as shown in Figure 3. A strong decrease of the intersubband spin relaxation matrix elements with shear strain increased is demonstrated in Figure 4. The relaxation decreases for all three values of the film thickness. This decrease is a consequence of the fact that the subband splitting increases with shear strain [3]. As soon as the intersubband splitting becomes larger than the spin-orbit interaction strength characterized by $\Delta_{SO}\sqrt{k_x^2 + k_y^2}$, the mixing of up- and down-spin states caused by this spin-orbit interaction is reduced.

3. Conclusion

The analytical approach for analyzing the spin properties of the thin silicon films has been developed. We demonstrated that the intersubband matrix elements decrease rapidly with shear strain.

This work is supported by the European Research Council through the grant #247056 MOSILSPIN.

References

- [1] Y. Song, H. Dery, Phys.Rev.B **86**, 085201 (2012).
- [2] G.L. Bir, G.E. Pikus, Symmetry and strain-induced effects in semiconductors. New York/Toronto: J. Wiley & Sons 1974.
- [3] V. Sverdlov, Strain-induced effects in advanced MOSFETs. Wien - New York. Springer 2011.
- [4] D. Osintsev *et al.*, Proceedings of the 15th International Workshop on Computational Electronics (2012).
- [5] M. Fischetti *et al.*, J. Appl. Phys., **94**, 1079 (2003).

$$\Psi_1 = \frac{1}{2} \left[(X_{11} + X'_{21}) + (X_{11} + X'_{21}) \frac{k_x - ik_y}{\sqrt{k_x^2 + k_y^2}} \right], \Psi_2 = \frac{1}{2} \left[(X_{11} + X'_{21}) - (X_{11} + X'_{21}) \frac{k_x - ik_y}{\sqrt{k_x^2 + k_y^2}} \right],$$

$$\Psi_3 = \frac{1}{2} \left[(X_{11} - X'_{21}) + (X_{11} - X'_{21}) \frac{k_x - ik_y}{\sqrt{k_x^2 + k_y^2}} \right], \Psi_4 = \frac{1}{2} \left[(X_{11} - X'_{21}) - (X_{11} - X'_{21}) \frac{k_x - ik_y}{\sqrt{k_x^2 + k_y^2}} \right].$$

$$X_1 = \Psi_1 \cos\left(\frac{\theta}{2}\right) - i \Psi_3 \sin\left(\frac{\theta}{2}\right), X_2 = \Psi_2 \cos\left(\frac{\theta}{2}\right) + i \Psi_4 \sin\left(\frac{\theta}{2}\right),$$

$$X_3 = \Psi_3 \cos\left(\frac{\theta}{2}\right) - i \Psi_1 \sin\left(\frac{\theta}{2}\right), X_4 = \Psi_4 \cos\left(\frac{\theta}{2}\right) + i \Psi_2 \sin\left(\frac{\theta}{2}\right),$$

$$\text{where } \tan(\theta) = \frac{\Delta_{SO} \sqrt{k_x^2 + k_y^2}}{D\varepsilon_{xy} - \frac{\hbar^2 k_x k_y}{M}}.$$

$$H = \begin{pmatrix} \frac{\hbar^2 k_x^2}{2m_l} + \frac{\hbar^2(k_x^2 + k_y^2)}{2m_t} - \delta & 0 & \frac{\hbar^2 k_0 k_z}{m_l} & 0 \\ 0 & \frac{\hbar^2 k_x^2}{2m_l} + \frac{\hbar^2(k_x^2 + k_y^2)}{2m_t} - \delta & 0 & \frac{\hbar^2 k_0 k_z}{m_l} \\ \frac{\hbar^2 k_0 k_z}{m_l} & 0 & \frac{\hbar^2 k_x^2}{2m_l} + \frac{\hbar^2(k_x^2 + k_y^2)}{2m_t} + \delta & 0 \\ 0 & \frac{\hbar^2 k_0 k_z}{m_l} & 0 & \frac{\hbar^2 k_x^2}{2m_l} + \frac{\hbar^2(k_x^2 + k_y^2)}{2m_t} + \delta \end{pmatrix}, \quad (1)$$

$$\text{where } \delta = \sqrt{\left(D\varepsilon_{xy} - \frac{\hbar^2 k_x k_y}{M}\right)^2 + \Delta_{SO}^2 (k_x^2 + k_y^2)}.$$

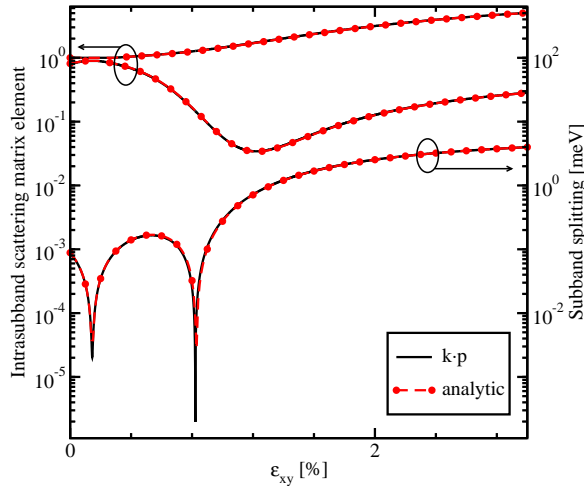


Fig.1: Intrasubband scattering matrix elements normalized to their values at zero strain for the film thickness 1.36nm for $k_x = 0.25\text{nm}^{-1}$ and $k_y = 0.25\text{nm}^{-1}$, and subband splitting as a function of shear strain

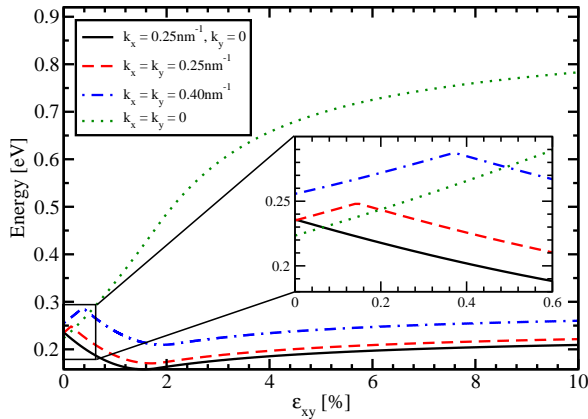


Fig.2: Energy for the first subband as a function of shear strain for the film thickness 1.36nm for the wave vectors \mathbf{k} (0.25nm^{-1} , 0), (0.25nm^{-1} , 0.25nm^{-1}), and (0.4nm^{-1} , 0.4nm^{-1}) and minimum energy in the second subband ($k_x = 0$ and $k_y = 0$)

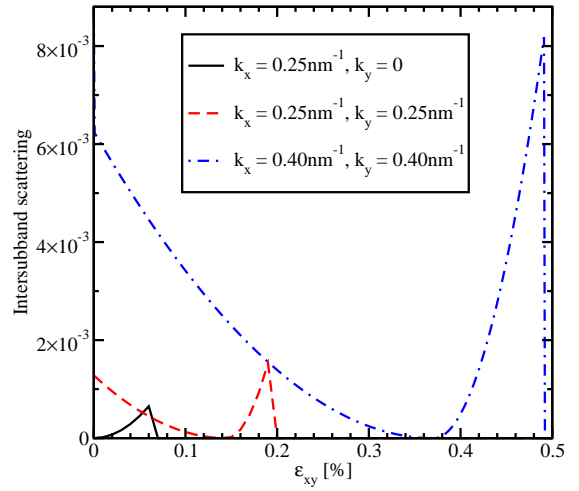


Fig.3: Intersubband scattering matrix elements normalized to the intrasubband scattering for zero strain between the states with the same spin projection for the film thickness 1.36nm

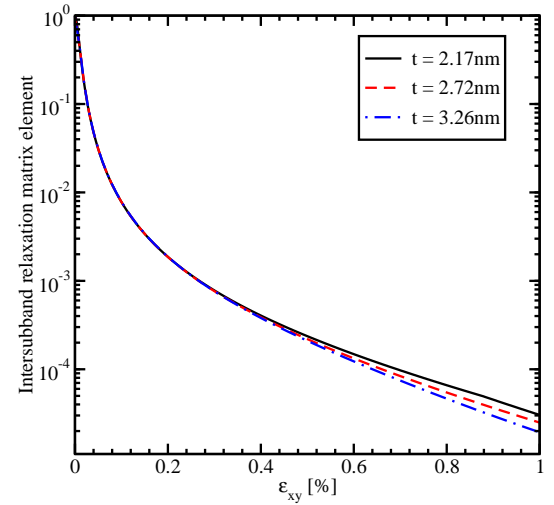


Fig.4: Normalized intersubband spin relaxation matrix elements as a function of shear strain for several values of the film thickness, for $k_x = 1\text{nm}^{-1}$ and $k_y = 0$